Nanoscale surface modifications and formation of conical structures at aluminum surface induced by single shot exposure of soft x-ray laser pulse

Masahiko Ishino,[1,a)] Anatoly Ya. Faenov,[1,2] Momoko Tanaka,[1] Noboru Hasegawa,[1] Masaharu Nishikino,[1] Satoshi Tamotsu,[3] Tatiana A. Pikuz,[1,2] Nail A. Inogamov,[4] Vasily V. Zhakhovsky,[2,5] Igor Yu. Skobelev,[2] Vladimir E. Fortov,[2] Viktor A. Khohlov,[4] Vadim V. Shepelev,[6] Toshiyuki Ohba,[1] Takeshi Kaihori,[1] Yoshihiro Ochi,[1] Takashi Imazono,[1] and Tetsuya Kawachi[1]

[1]*Kansai Photon Science Institute, Japan Atomic Energy Agency, Kyoto 619-0215, Japan*
[2]*Joint Institute for High Temperatures, Russian Academy of Science, Moscow 125412, Russia*
[3]*Graduate School of Humanities and Science, Nara Women's University, Nara 630-8506, Japan*
[4]*Landau Institute for Theoretical Physics, Russian Academy of Science, Chernogolovka 142432, Russia*
[5]*Department of Physics, University of South Florida, Tampa, Florida 33620-5700, USA*
[6]*Institute for Computer Aided Design, Russian Academy of Science, Moscow 123056, Russia*

(Received 4 October 2010; accepted 9 November 2010; published online 4 January 2011)

We irradiated the soft x-ray laser (SXRL) pulses having a wavelength of 13.9 nm, a duration time of 7 ps, and fluences of up to 27 mJ/cm^2 to aluminum (Al) surface. After the irradiation process, the modified surface was observed with the visible microscope, the scanning electron microscope, and the atomic force microscope. The surface modifications caused by the SXRL pulses were clearly seen, and it was found that the conical structures having about 70–150 nm in diameters were formed under a single pulse shot. The conical structures were formed in the features with the average depth of about 40 nm, and this value was in accordance with the attenuation length of the SXRL beam for Al. However, those conical structures were deconstructed under the multiple pulse shots exposure. Thermomechanical modeling of SXRL laser interaction with Al surface, which explains nanostructure surface modification, was provided. © *2011 American Institute of Physics*.
[doi:10.1063/1.3525980]

I. INTRODUCTION

Laser pulses having short duration times of picosecond or femtosecond have abilities to make high temperature and pressure, excite states of electrons in materials, and emit rays, as the results of interaction with matters.[1] Soft x-ray laser (SXRL) is one of attractive x-ray source for scientific studies, because of its features of highly spatial coherence, short duration time, and short wavelength.[2] The highly spatial coherence is applicable to observe a surface topography, a density distribution of plasma, and a diffraction pattern of object. The short duration time enables us to measure temporal phenomena by means of a time resolution technique. The emission of short wavelength in soft x-ray region, i.e., photon energy of soft x-ray is higher than that of visible light, has ability to photoionize element with one photon.

At the Japan Atomic Energy Agency (JAEA), we have generated a SXRL beam having a wavelength of 13.9 nm.[3–6] Since this SXRL beam has a large output energy of near 1 $\mu J/pulse$, a fully spatial coherence, and a short duration time of 7 ps,[7–9] many application researches using phenomenal features of the SXRL pulse have been done. The speckle pattern and interference pattern measurements were the research techniques using the features of a spatial coherence and a short duration time of the SXRL pulses.[10–15] The evaluation of interaction of Xe clusters with the SXRL pulse was the research using an advantage not only of the short wavelength of the beam but also of the large number of photons in the pulse.[16]

Recently, we investigated a characteristic and intensity distribution of the focal patterns of SXRL pulses by means of color center formation in LiF crystal,[17] and the ablation property of LiF crystal was also studied experimentally[18] and theoretically.[19,20] Our experiments revealed that the value of ablation threshold obtained with the focused 13.9 nm, 7 ps SXRL pulse is much smaller than those obtained with other lasers having longer pulse durations and/or longer wavelengths. The low ablation threshold of a material for a SXRL beam has a possibility of efficient nanometer size machining by an ablation process and by a lithography method, but the SXRL pulse will break an expensive mask pattern or a substrate very easily. Hence, we are interested in a pursuit of ablation process or mechanism for material induced by an irradiation of SXRL pulse.

In this article, we report the surface modification of metal aluminum (Al) surface by the irradiation of the SXRL pulses. To analyze the surface modifications induced by the SXRL pulse irradiations, the irradiated surface were observed with a visible microscope, a scanning electron microscope (SEM), and an atomic force microscope (AFM). Under the single shot irradiation, we found that a formation of the conical nanometer size structures is occurred.

II. EXPERIMENT

The SXRL irradiation experiment was carried out by use of the SXRL facility at JAEA. The experimental setup was

a)Electronic mail: ishino.masahiko@jaea.go.jp.

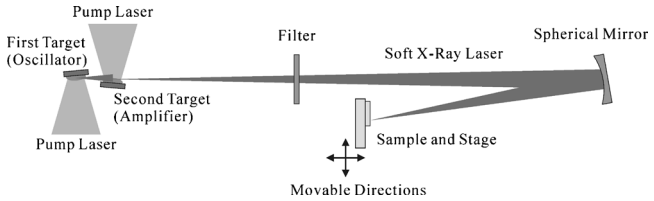

FIG. 1. Schematic diagram of experimental setup for irradiation of a focusing SXRL pulse to a sample surface. Sample stage moves in a plane.

composed of three elements; the SXRL source, optics, and the sample. A schematic diagram of the experimental setup is shown in Fig. 1.

The spatially coherent SXRL pulse was generated from the silver (Ag) plasma mediums using an oscillator-amplifier configuration with Ag double targets.[4,5] The Ag tapes were used as the plasma targets,[21] and the tape targets were irradiated by the linearly focusing laser pulses generated from a chirped pulse amplification glass laser system with zigzag slab Nd:glass amplifiers.[22] The soft x-ray seed light generated by the first Ag plasma was amplified with the second Ag plasma. Characteristics of the generated SXRL from Ag double targets had a wavelength of 13.9 nm, bandwidth of narrower than 10^{-4}, duration time of 7 ps, and beam divergence of 0.35 mrad (H) $\times$ 0.3 mrad (V). The SXRL system worked in 0.1 Hz regime, and, in addition, the output energy of the order of microjoules was achieved. The details of the SXRL generation are described in Ref. 23 and references in it.

The SXRL pulse was focused on the sample surface by using a spherical Mo/Si multilayer coated mirror having a radius of 1000 mm in curvature. The output energy of the SXRL pulse was varied in each shot, but the average output energy of the SXRL pulse was estimated to be about 200 nJ.[23] The spherical Mo/Si multilayer coating was optimized for soft x-rays of 13.9 nm at an incidence angle of 2°, and it placed at a distance of 2637 mm from the SXRL output. A Zr filter having 0.2 μm thickness was placed in front of the spherical mirror to reduce the scattered optical radiations from the laser produced Ag plasmas. The transmittance of the Zr filter and the reflectivity of the Mo/Si mirror for soft x-rays of 13.9 nm were about 48% and about 50%, respectively. Therefore, the total energy of the SXRL beam on the sample surface was about 48 nJ. Al plate with a thickness of 2.5 mm was used as the sample, and the sample was mounted on the sample holder having two movable directions. The Al surface was moved after the prescribed number of shots along the propagation direction of incident SXRL beam around the best focal position and it was also moved in the perpendicular to the propagation direction to irradiate the fresh Al surface. All the irradiation process described above was carried out in a vacuum chamber.

After the irradiation, the Al surface was observed by use of a visible microscope (BX60, OLYMPUS Corporation) to confirm that the irradiated positions were something modified or not. The detail of structures of modified surface, which could not see with a visible microscope, was observed by a SEM (JSM-6380LVN, JEOL Ltd.). The cross sectional profiles of the induced patterns, also whole images of patterns, were measured by an AFM (Explorer, TopoMetrix Corporation).

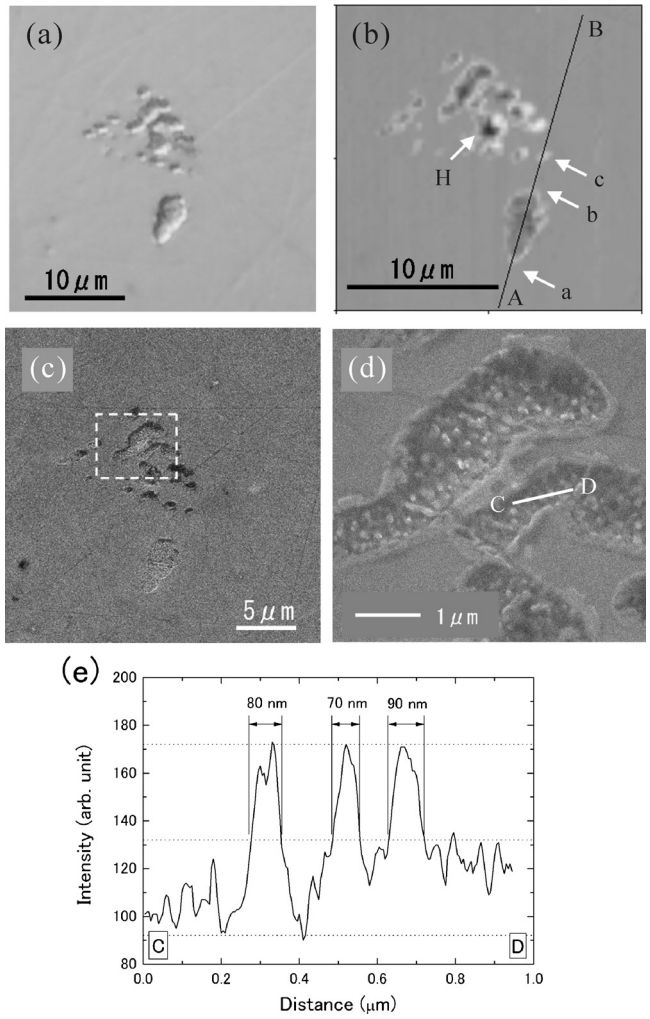

FIG. 2. Images of the irradiated surface after a single laser shot of the SXRL beam near the best focus position obtained with (a) microscope with DIC mode, (b) AFM, and (c) SEM, (d) magnified image with SEM, and (e) trace along modified surface area. Line A–B, and Line C–D show the analysis positions of a cross sectional profiles. Arrow H shows the ablated hole, and arrows a, b, and c are the rims of the features.

III. RESULT AND DISCUSSION

Figure 2(a) shows the irradiated surface after a single laser shot of the SXRL beam near the best focus position observed by the visible microscope with the differential interference contrast (DIC) mode. Figures 2(b) and 2(c) are AFM and SEM images of the same position shown in Fig. 2(a). The surface modification caused by the SXRL pulse irradiation, which is different from the original surface, is clearly observed. The observed surface is composed of a several features. The features are dispersed in an area of 11 μm $\times$ 16 μm. The distribution of features will represent the distribution of the gain structures in Ag plasmas at this experiment series, because the spherical mirror reconstructs a reduction image of the SXRL source (see Fig. 1). A magnified SEM image of the features at the area shown with square in Fig. 2(c) is presented in Fig. 2(d). In the SEM images, the

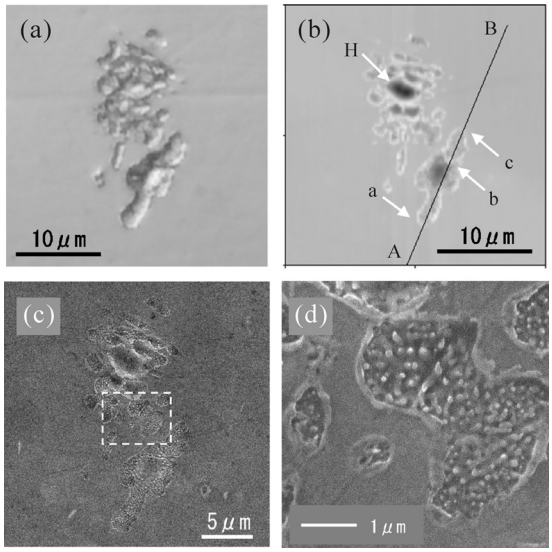

FIG. 3. Images of the irradiated surface after a single laser shot of the SXRL beam at the position of +0.5 mm away from the focal position. Figures are obtained in the same manner as shown in Figs. 2(a)–2(d).

fine structures existing in the features, which were scarcely seen in the DIC observation, can be seen clearly. Two types of the modified structures can be confirmed. One is the ablated structures, e.g., deep hole pointed out with arrow H in Fig. 2(b). The depth of the deep hole is evaluated to be 165 nm by AFM measurement. The other is the shallow features containing the conical structures. Judging from the scale bar inserted in Fig. 2(d) and the cross sectional profile shown as line C–D in Fig. 2(e), the each conical structure has a diameter of 70–150 nm.

The observed DIC, AFM, and SEM images of the irradiated surface after a single SXRL shot at the position of +0.5 mm away from the focal position are presented in Figs. 3(a)–3(d) in the same manner as shown in Figs. 2(a)–2(d). The features caused by the SXRL pulse irradiation are also observed, and those are dispersed in an area of 11 μm $\times$24 μm. The difference of dispersed area might represent the astigmatism due to the 2° incidence angle of the spherical mirror. In Figs. 3(b) and 3(c), the large ablation areas are seen, and the depth of the ablated hole, shown with arrow H, is measured to be 380 nm. The evaluated depth in Fig. 3(b) is larger than that in Fig. 2(b). It would be thought that the more intense SXRL pulse was irradiated to the surface at this position. However, in Fig. 3(d), the conical structures observed as same as those in Fig. 2(d) are also seen. It can be seen especially in Figs. 3(b) and 3(c), the conical structures exist around the ablated hole, i.e., the conical structures are formed by the SXRL pulses with the weak fluence less than the ablation threshold. The both conical structures observed in Figs. 2(d) and 3(d) have uniform shapes and formed closely in the shallow features.

Shown in Figs. 4(a) and 4(b) are the cross sectional profiles of the features derived from the AFM measurements. The analyses positions are shown as line A–B shown in Figs. 2(b) and 3(b), respectively. These two features exist at the relatively same positions and are similar shape. These features would be irradiated with the SXRL beams generated

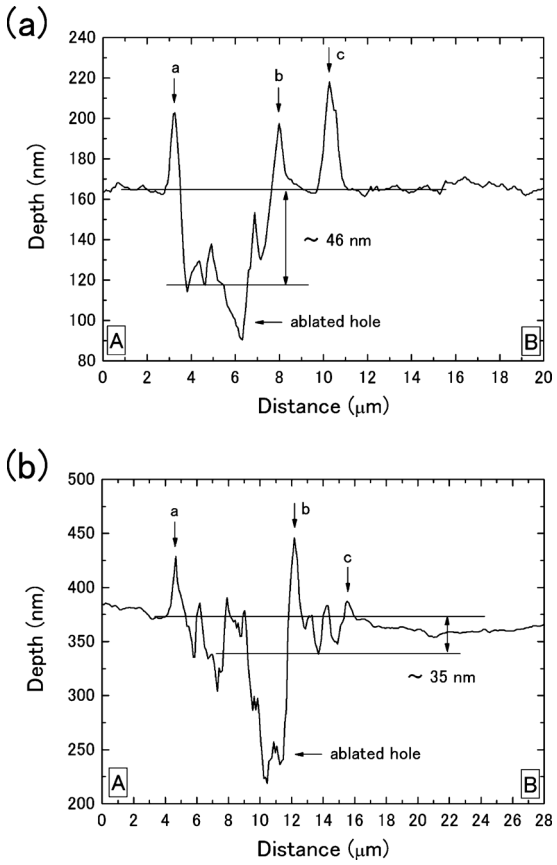

FIG. 4. Cross sectional profiles of the modified surfaces (a) at the line A–B shown in Figs. 2(b) and (b) that in Fig. 3(b). Arrows a, b, and c are the rims of the features shown in Figs. 2(b) and 3(b).

from the same gain region in the Ag plasmas. The profiles shown with arrows a, b, and c in Figs. 4(a) and 4(b) are the rims of the features, which are also shown with arrows in Figs. 2(b) and 3(b). The average depth of the features having the conical structures was evaluated to be around 40 nm, which was in accordance with the attenuation length of 37 nm for soft x-rays of 13.9 nm for Al. As the result of the interaction between the SXRL beam and Al surface, the conical structures are formed within an attenuation length.

In this work, it reveals that the conical structures are formed by the irradiation of the SXRL pulse with the fluence less than the ablation threshold. The fluence is calculated to be 18–27 mJ/cm^2 at a single shot, because the irradiated areas estimated from the dispersions of the features are 1.76×10^{-6} cm^2 and 2.64×10^{-6} cm^2. In the previous work, it was pointed out that only 6% of the SXRL energy was concentrated to the best focal spot.[17,18] However, using the LiF detector technique for estimation of quality of the SXRL beam and its focusing properties, we found that the SXRL energy concentration in the best focusing spot reached about 40% in this experiment series. Such strong enhancement of the SXRL beam focusing properties was achieved due to using better quality of a spherical mirror more than that of the previous. If the best focal spots would mean the ablation holes, the flux of 7.3–11 mJ/cm^2 might be concentrated on the ablated hole positions. Anyway, the ablation threshold of Al for the SXRL beam would be in the range of 7.3–27 mJ/cm^2.

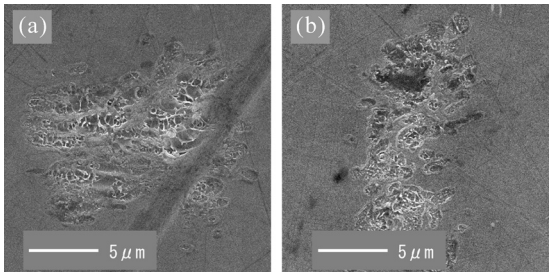

FIG. 5. SEM images of the irradiated surface after ten laser shots of the SXRL beam at the position of (a) near the best focus and (b) +0.5 mm away from the focus.

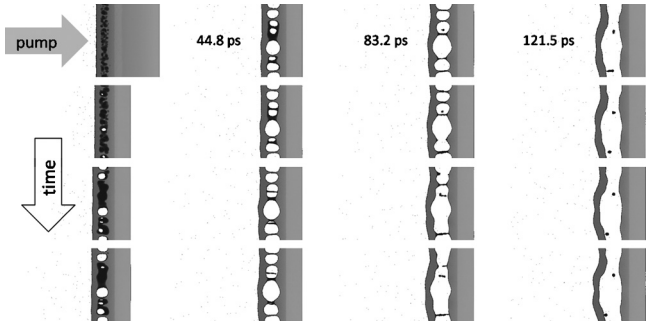

FIG. 6. Appearance of runaway layer in laser ablation for thin heated depth. The wide Al target with transverse dimension $L=122$ nm, heated up to the $T_0(0)=3.9$ kK at the small heated depth $d_T=18.6$ nm. Time step between frames is 6.4 ps.

Formations of the conical structures induced by multiple photon pulse irradiations (including infrared, ultraviolet, and soft x-ray) were reported in some literatures[24–26] and also seen in etched structure.[27] The conical structures induced with the infrared laser pulses had relatively large diameter of micrometer order in spite of the sample materials (silicon, polymer).[24,25] Moreover, the conical structures grew with the increasing the irradiated total flux.[24–26] Figures 5(a) and 5(b) show the irradiated surface after ten laser shots of the SXRL pulses at the position of near the best focus and +0.5 mm away from the focus, respectively. The conical structures were destroyed under the multiple laser shots, and no growth can be seen. The formation of the conical nanometer size structures on Al surface with a single shot pulse might be the characteristic of the SXRL pulse.

A model simulation will help us to draw a process of the surface modification. There are the following main processes, which are important to discuss for better understanding of surface modification by SXRL pulse. Short laser pulse with pulse duration τ less or of the order of the acoustic time $t_s=d_T/c_s$ increases pressure inside the heated layer, here d_T and c_s are the laser heat penetration depth and sonic speed.[19,28,29] Sometimes, it is said that the short pulse "loads" a target. There is an important thermomechanical link connecting energy absorption, pressure rise, and hydrodynamic response of a target. Thermomechanical response replaces evaporative ablation, usual for laser-matter interaction, to thermomechanical ablation.[19,20,29] In the latter case, evaporative break of cohesive bonds between atoms is replaced by mechanical fragmentation of initially continuous target when the amplitude of tensile stress overcomes material strength. In mechanics of solids, this process is called spallation. It is caused by unloading of high pressure layer of a target.

Spallation has sharp threshold at fluence, since this kind of ablative removal of matter appears only if the tensile stress, proportional to absorbed fluence, overcomes the finite value of cohesive strength of condensed matter (material strength).[20] Near threshold the efficiency of material removal, evaluated as the ratio of amount of ablated mass per absorbed energy, is higher for short pulses in comparison with long pulses and as it was demonstrated in the previous works should be extremely low (~ 10 mJ/cm^2) for dielectrics.[18–20] Since the heat depths are $d_T \sim 10-100$ nm and sound speed c_s is a few kilometers persecond then typical $t_s \sim 10$ ps. Therefore the short pulses have durations in the few picosecond range (as it is in our experimental case ~ 7 ps) and shorter, while long pulses have nanosecond and longer durations. It means that in our experiments in some vicinity above the threshold the spallative removal of matter dominates above the evaporative removal.

SXRL pulse excites an electronic subsystem of condensed state and thus induces a chain of relaxation processes in which the electronic and ionic subsystems relax to a new thermodynamic equilibrium. In one type of problems, the relaxation (relaxation time: t_{rel}) is finished significantly before the acoustic response proceeds $t_{rel} \ll t_s$ (fast relaxation). In another case, the relaxation lasts longer $t_{rel} \sim t_s$ or $t_{rel} > t_s$. The first case is simple, because the calculations of pressure become necessary, when local electron and ion temperatures are equal (the electron and ion subsystems return to equilibrium). The spatial structure of the pressure field becomes important at the dynamic stage at the time interval $t \sim t_s$. This is the case of the first class mentioned above, when system transfers to equilibrium before the beginning of the dynamical stage. In this equilibrium case, the pressure is calculated from the known equilibrium thermodynamic relations between pressure and density and internal energy. In the second type, it is necessary to evaluate influence of excited electrons onto material strength and pressure. Excited electrons in metals are usually described in the Fermi approximation.[9,29] There are the quantum-mechanical simulations devoted to calculations of influence of electronic excitations to material strength.[30,31] These calculations show that in case of metals the excitations rather weakly change melting temperature and phonon spectra.

As it was demonstrated previously,[19,28,32] a short SXRL pulse under interaction with matter initiates a sequence of stages: (i) release or unloading, (ii) metastable state, (iii) nucleation, and (iv) evolution of foam. Nucleation takes place if the absorbed fluence is above the nucleation threshold F_{nucl}. It is important that nucleation does not mean tacitly that spallative plate will run away. The spallative ablation threshold F_{abl} and F_{nucl} are separated. The separation $(F_{abl}-F_{nucl})/F_{abl}$ belongs to the few percent range. As was shown in Refs. 19, 28, and 32, that during the release, the internal foam layer inflates (in the direction normal to the target surface) to the thickness comparable to the distance separating the foam layer and the free surface of the target. Therefore, as it is shown in Figs. 6 and 7(a)–7(d), the foam layer per-

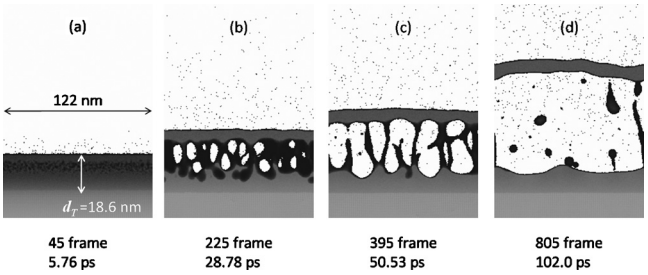

FIG. 7. Three main stages of nanomodification of Al surface under SXRL pulse irradiation. Multiple nucleation (a) and further evolution of the foam layer [(b)–(d)]. More deep contrast marks the molten Al. Growing foams perturb the free surface above (b) and (c). This free surface separates condensed layer from vapor. Between the free surface and the foam layer, the spallative layer is formed. As the foams inflate further, the threads, connecting spallative layer and the bulk of a target, break off, and the spallative layer runs away (d).

turbs the free surface, causing appearance of the surface nanorelief.

Development of the nanorelief is a dynamical phenomenon, caused by deceleration of the free surface, inflation of foam, and the surface tension resistance to the inflation. There is the appearance time t_{appr} when it develops. This time is larger than t_s because fluence F is $\approx F_{abl}$, and the nanorelief appears near the stopping point of the free surface, when this surface is almost stopped by the material resistance to the stretching. Expansion velocities at this stage are small, and the nanorelief develops slowly.

In Al and in many other materials, the ablation threshold F_{abl} is higher than the melting threshold F_{melt}, and then at $F > F_{nucl}$ foams appears inside the molten layer. There are two cases with slow development of foam: one when $F_{nucl} < F_{abs} < F_{abl}$ and another when F_{abs} is slightly above F_{abl}, here F_{abs} is the absorbed fluence by material. In the first case, the foam remains closed under the surface.[19,28,32] In the second case, there is the process of slow detachment of the spallative layer. The layer is connected by the random net of the liquid threads or filaments with the bulk of a target through the foam layer. The filaments are stretched and break off one after another during detachment of the spallative layer. During this process, a nanobrush from a forest of standing filaments appears. Cooling due to electron heat conduction is important. In a liquid state, the foam under the target surface $F < F_{abl}$ and the nanobrush $F > F_{abl}$ finally disappears because the surface tension collapses foams with low vapor pressure in the foam and smooths down the threads and the surface bumps. Foams collapse under action of surface tension when the tensile stress, decelerating the spallative layer and thus supporting the foams, decreases to zero. Contrary to this smoothing, the undersurface foams $F < F_{abl}$ and nanobrush $F > F_{abl}$ remain in the final relief if conductive loses are fast enough to freeze them before they smoothed by surface tension.[20,28,32] The nanobrush may be accompanied with frozen foams under the surface.

To model nanomodification of surface by irradiation of SXRL pulse, we developed molecular dynamic (MD) code.[19,20,28,32] Simulations of the development of the foam and its freezing require huge computer power and smart multiprocessors algorithm, because foam occupies large volume and inflation/freezing processes are very slow. In our modeling, in order to include the electron thermal conductivity into the MD code, the electrons as classical particles were added to the atom subsystem. Each electron is assumed to associate with its host atom/ion. An electron always allocates the position of host, but it has its own velocity. The neighboring atoms may exchange their electrons with some frequency, determined from the known experimental thermal conductivity of liquid aluminum at the melting point.[30,32] It is important that in case of the foam our method allows us to describe spatial separation of thermal fluxes pumping heat through the threads and walls with small cross-section.[19] This greatly delays cooling through the foam. Therefore, the base of the foam, which is located from the bulk side of a target, cools faster than the film between the foam and free surface.

If summarize our modeling demonstrated that the three stages of evolution of the Al nanofoam could be distinguished. These stages are presented in Figs. 7(a)–7(d): nucleation of the interatomic size foams Fig. 7(a), inflation of the foams Figs. 7(b) and 7(c), and run away Fig. 7(d), of the spallative layer. We would like to stress that the important result of our modeling is demonstration that the size of surface nanorelief develops is in the scale of ten's of nanometers, which are in a good agreement with experimental results.

At the last, we point out that the photon energy of the SXRL beam is slightly higher than the *L*-absorption edge of Al (E=73 eV), so that the innershell ionization and the generation of the photoelectrons will occur efficiently.

IV. CONCLUSION

We irradiated Al surface with the SXRL pulses with a wavelength of 13.9 nm and a duration time of 7 ps, and the fluences of the SXRL pulses were calculated to be up to 27 mJ/cm^2. At the irradiated surface, we found that the ablation holes and the conical structures were formed in the focused patterns by single shot exposure of the SXRL pulse. The conical structures having the diameters of 70–150 nm were formed in the modified surfaces corresponding with low fluence areas. The average depth of modified surfaces was around 40 nm, which was in accordance with the attenuation length of SXRL beam to Al target. Our thermomechanical approach for modeling of SXRL pulse interaction with Al allowed to demonstrate the crucial role of shortening of laser pulses and explain nanomodification of surface in experiments.

In this work, we demonstrated that the nanofabrication of Al surface could be provide in the single laser shot under the very low SXRL fluence, which were essentially lower comparing with nanofabrication by visible or infrared laser pulses. The quality of the produced nanostructures strictly depends on the homogeneity of the SXRL beam and particular on the quality of the focusing mirror. We did not optimize yet these parameters. In our future investigations, we could do such optimization and it will allow us to fabricate high quality homogeneous nanostructures. However, in our investigations, the modified Al surface induced by the exposure of SXRL pulse has the depths of about 40 nm. The wavelength

of the SXRL beam is shorter than those of visible lights, and then, potentially the SXRL beam has an ability to draw small patterns, such as grooves or channels with nanometer order width, on surfaces of materials. Then, the SXRL beam would be a candidate for a tool of micromachining, which enable to fabricate of three dimensional structures with nanometer size on material surfaces.

The result we demonstrated in this work will be important not only for a pursuit of ablation process but also for future application of SXRL beam such as micromachining.

ACKNOWLEDGMENTS

This work was partly supported by Grant-in-Aid for Scientific Research (B) under Grant No. 21360364 (2009), from the Ministry of Education, Culture, Sports, Science, and Technology (MEXT), Japan. Part of the work was supported by the Russian Foundation for Basic Research (RFBR) (Grant Nos. 10-02-91174 GFEN_a, 10-02-00345a, and 10-02-00434a), and by the Russian Academy of Science (RAS) Presidium Program of Basic Research 2 and 21.

[1]See for example, J. J. Duderstadt and G. A. Moses, *Inertial Confinement Fusion* (Wiley, New York, 1982); I. C. E. Turcu and J. B. Dance, *X-rays from Laser Plasmas* (Wiley, New York, 1998).
[2]P. Jaeglé, *Coherent Sources of XUV Radiation: Soft x-ray Lasers and High-Order Harmonics Generation*, Springer Series in Optical Science Vol. 106 (Springer, New York, 2006).
[3]T. Kawachi, M. Kado, M. Tanaka, A. Sasaki, N. Hasegawa, A. V. Kilpio, S. Namba, K. Nagashima, P. Lu, K. Takahashi, H. Tang, R. Tai, M. Kishimoto, M. Koike, H. Daido, and Y. Kato, Phys. Rev. A **66**, 033815 (2002).
[4]M. Tanaka, M. Nishikino, T. Kawachi, N. Hasegawa, M. Kado, M. Kishimoto, K. Nagashima, and Y. Kato, Opt. Lett. **28**, 1680 (2003).
[5]M. Nishikino, N. Hasegawa, T. Kawachi, H. Yamatani, K. Sukegawa, and K. Nagashima, Appl. Opt. **47**, 1129 (2008).
[6]N. Hasegawa, T. Kawachi, T. Utsumi, A. Sasaki, M. Tanaka, M. Kado, K. Sukegawa, P. Lu, M. Kishimoto, R. Tai, K. Nagashima, M. Koike, H. Daido, and Y. Kato, Jpn. J. Appl. Phys., Part 1 **43**, 2519 (2004).
[7]M. Nishikino, M. Tanaka, K. Nagashima, M. Kishimoto, M. Kado, T. Kawachi, K. Sukagawa, Y. Ochi, N. Hasegawa, and Y. Kato, Phys. Rev. A **68**, 061802(R) (2003).
[8]M. Nishikino, M. Tanaka, Y. Ochi, M. Kishimoto, M. Ishino, N. Hasegawa, M. Kado, K. Sukagawa, T. Kawachi, and K. Nagashima, IEEE J. Sel. Top. Quantum Electron. **10**, 1382 (2004).
[9]Y. Ochi, T. Kawachi, N. Hasegawa, A. Sasaki, K. Nagashima, K. Sukegawa, M. Kishimoto, M. Tanaka, M. Nishikino, and M. Kado, Appl. Phys. B: Lasers Opt. **78**, 961 (2004).
[10]R. Z. Tai, K. Namikawa, M. Kishimoto, M. Tanaka, K. Sukegawa, N. Hasegawa, T. Kawachi, M. Kado, P. Lu, K. Nagashima, H. Daido, H. Murayama, A. Sawada, M. Ando, and Y. Kato, Phys. Rev. Lett. **89**, 257602 (2002).
[11]R. Z. Tai, K. Namikawa, A. Sawada, M. Kishimoto, M. Tanaka, P. Lu, K. Nagashima, H. Murayama, and M. Ando, Phys. Rev. Lett. **93**, 087601 (2004).
[12]H. Tang, O. Guilbaud, G. Jamelot, D. Ros, A. Kilisnick, D. Joyeux, D. Phalippou, M. Kado, M. Nishikino, M. Kishimoto, K. Sukegawa, M. Ishino, K. Nagashima, and H. Daido, Appl. Phys. B: Lasers Opt. **78**, 975 (2004).
[13]K. Namikawa, M. Kishimoto, K. Nasu, E. Matsushita, R. Z. Tai, K. Sukegawa, H. Yamatani, H. Hasegawa, M. Nishikino, M. Tanaka, and K. Nagashima, Phys. Rev. Lett. **103**, 197401 (2009).
[14]N. Hasegawa, Y. Ochi, T. Kawachi, K. Terakawa, T. Tomita, M. Yamamoto, M. Nishikino, T. Ohba, T. Kaihori, T. Imazono, A. Sasaki, M. Kishimoto, M. Ishino, M. Kado, M. Tanaka, T. Nakazato, N. Sarukura, and T. Suemoto, "Development of the x-ray interferometer and the method of spatial and temporal synchronization of XRL and optical pulse," Springer Proceedings in Physics, Proceedings of X-Ray Lasers 2010 (in press).
[15]T. Suemoto, K. Terakawa, Y. Ochi, T. Tomita, M. Yamamoto, N. Hasegawa, M. Deki, Y. Minami, and T. Kawachi, Opt. Express **18**, 14114 (2010).
[16]S. Namba, N. Hasegawa, M. Nishikino, T. Kawachi, M. Kishimoto, K. Sukegawa, M. Tanaka, Y. Ochi, K. Takiyama, and K. Nagashima, Phys. Rev. Lett. **99**, 043004 (2007).
[17]A. Ya. Faenov, Y. Kato, M. Tanaka, T. A. Pikuz, M. Kishimoto, M. Ishino, M. Nishikino, Y. Fukuda, S. V. Bulanov, and T. Kawachi, Opt. Lett. **34**, 941 (2009).
[18]A. Ya. Faenov, N. A. Inogamov, V. V. Zhakhovskii, V. A. Khokhlov, K. Nishihara, Y. Kato, M. Tanaka, T. A. Pikuz, M. Kishimoto, M. Ishino, M. Nishikino, T. Nakamura, Y. Fukuda, S. V. Bulanov, and T. Kawachi, Appl. Phys. Lett. **94**, 231107 (2009).
[19]N. A. Inogamov, A. Ya. Faenov, V. A. Khokhlov, V. V. Zhakhovskii, Yu. V. Petrov, I. Yu. Skobelev, K. Nishihara, Y. Kato, M. Tanaka, T. A. Pikuz, M. Kishimoto, M. Ishino, M. Nishikino, Y. Fukuda, S. V. Bulanov, T. Kawachi, S. I. Anisimov, and V. E. Fortov, Contrib. Plasma Phys. **49**, 455 (2009).
[20]N. A. Inogamov, V. V. Zhakhovskii, A. Ya. Faenov, V. V. Shepelev, I. Y. Skobelv, V. A. Khokhlov, Y. Kato, M. Tanaka, T. A. Pikuz, M. Kishimoto, M. Ishino, M. Nishikino, Y. Fukuda, S. V. Bulanov, T. Kawachi, Y. V. Petrov, S. I. Anisimov, and V. E. Fortov, Appl. Phys. A: Mater. Sci. Process. **101**, 87 (2010).
[21]M. Nishikino, Y. Ochi, N. Hasegawa, T. Kawachi, and H. Yamatani, Rev. Sci. Instrum. **80**, 116102 (2009).
[22]Y. Ochi, N. Hasegawa, T. Kawachi, and K. Nagashima, Appl. Opt. **46**, 1500 (2007).
[23]Y. Ochi, T. Kawachi, N. Hasegawa, M. Nishikino, T. Ohba, M. Tanaka, M. Kishimoto, T. Kaihori, K. Nagashima, and A. Sugiyama, Jpn. J. Appl. Phys. **48**, 120212 (2009).
[24]J. Bonse, S. Baudach, J. Krüger, W. Kautek, and M. Lenzer, Appl. Phys. A: Mater. Sci. Process. **74**, 19 (2002).
[25]N. S. Murthy, R. D. Prabhu, J. J. Martin, L. Zhou, and R. L. Headrick, J. Appl. Phys. **100**, 023538 (2006).
[26]A. Bartnik, H. Fiedorowicz, R. Jarocki, J. Kostecki, A. Szczurek, and M. Szczurek, Appl. Phys. B: Lasers Opt. **96**, 727 (2009).
[27]A. Bartnik, H. Fiedorowicz, R. Jarocki, L. Juha, J. Kostecki, R. Rakowski, and M. Szczurek, Appl. Phys. B: Lasers Opt. **82**, 529 (2006).
[28]V. Zhakhovskii, N. Inogamov, and K. Nishihara, J. Phys.: Conf. Ser. **112**, 042080 (2008).
[29]S. I. Anisimov, N. A. Inogamov, Y. V. Petrov, V. A. Khokhlov, V. V. Zhakhovskii, K. Nishihara, M. B. Agranat, S. I. Ashitkov, and P. S. Komarov, Appl. Phys. A: Mater. Sci. Process. **92**, 797 (2008).
[30]V. Recoules, J. Clerouin, G. Zerah, P. M. Anglade, and S. Mazevet, Phys. Rev. Lett. **96**, 055503 (2006).
[31]V. V. Stegailov, Contrib. Plasma Phys. **50**, 31 (2010).
[32]V. V. Zhakhovskii, N. A. Inogamov, and K. Nishihara, JETP Lett. **87**, 423 (2008).